

Automatic Grading of Individual Knee Osteoarthritis Features in Plain Radiographs using Deep Convolutional Neural Networks

Aleksei Tiulpin^{1,2,*} and Simo Saarakkala^{1,2}

¹Research Unit of Medical Imaging, Physics and Technology, University of Oulu, Oulu, Finland.

²Department of Diagnostic Radiology, Oulu University Hospital, Oulu, Finland

*aleksei.tiulpin@oulu.fi

ABSTRACT

Knee osteoarthritis (OA) is the most common musculoskeletal disease in the world. In primary healthcare, knee OA is diagnosed using clinical examination and radiographic assessment. Osteoarthritis Research Society International (OARSI) atlas of OA radiographic features allows to perform independent assessment of knee osteophytes, joint space narrowing and other knee features. This provides a fine-grained OA severity assessment of the knee, compared to the gold standard and most commonly used Kellgren-Lawrence (KL) composite score. However, both OARSI and KL grading systems suffer from moderate inter-rater agreement, and therefore, the use of computer-aided methods could help to improve the reliability of the process. In this study, we developed a robust, automatic method to simultaneously predict KL and OARSI grades in knee radiographs. Our method is based on Deep Learning and leverages an ensemble of deep residual networks with 50 layers, squeeze-excitation and ResNeXt blocks. Here, we used transfer learning from ImageNet with a fine-tuning on the whole Osteoarthritis Initiative (OAI) dataset. An independent testing of our model was performed on the whole Multicenter Osteoarthritis Study (MOST) dataset. Our multi-task method yielded Cohen's kappa coefficients of 0.82 for KL-grade and 0.79, 0.84, 0.94, 0.83, 0.84, 0.90 for femoral osteophytes, tibial osteophytes and joint space narrowing for lateral and medial compartments respectively. Furthermore, our method yielded area under the ROC curve of 0.98 and average precision of 0.98 for detecting the presence of radiographic OA ($KL \geq 2$), which is better than the current state-of-the-art.

Introduction

Osteoarthritis (OA) is the most common musculoskeletal disease leading to disability^{1,2}. The etiology of OA is not currently understood, it has no cure, and eventually leads to total knee replacement¹. Only available therapies for OA patients at the moment are behavioral interventions, e.g. weight loss, properly designed physical exercise and strengthening of joint muscles, which could lead to a temporary pain relief and decreasing OA progression rate³.

OA is currently diagnosed using clinical examination and almost always confirmed by radiography (X-ray imaging) that is a cheap and widely used imaging modality⁴. The gold standard radiographic knee OA severity measure is Kellgren-Lawrence (KL) grading system⁵. However, KL grade suffers from subjectivity of a practitioner and it is also a composite score not focusing separately on individual features as well as the side of OA (lateral or medial). A more recent and feature-specific approach to grade radiographic OA severity is Osteoarthritis Research Society International (OARSI) atlas⁶. Specifically, it enables grading of such features as femoral osteophytes (FO), tibial osteophytes (TO) and joint space narrowing (JSN) compartment-wise (see Figure 1). However, similar to KL score, OARSI grading suffers from subjectivity of the reader. Potentially, computer-aided methods based on Machine Learning (ML) could improve the situation by automating the OARSI grading similarly as it has been done for the KL grading⁴.

Deep Learning (DL) is a state-of-the-art ML approach that allows learning of features directly from the data, and it has recently revolutionized the field of medical image analysis by surpassing the conventional computer vision techniques that required manual engineering of data representation methods⁷. In the OA research field, several studies demonstrated success in the analysis of Magnetic Resonance Imaging (MRI) data^{8,9}, basic research¹⁰, prediction of knee osteoarthritis progression¹¹ and, in particular, automation of the KL-grading of knee and hip radiographs using deep convolutional neural networks (CNN)^{4,12-14}. However, only a few attempts have been made to assess individual knee OA features from plain radiography.

To the best of our knowledge, Oka *et al.*¹⁵ were the first to report automatic analysis of individual knee OA features. Later, Thomson *et al.* (2016)¹⁶ used a more robust setup and an advanced methodology based on the shape and texture descriptors to evaluate the presence of osteophytes and radiographic OA ($KL \geq 2$). The authors reported the area under the receiver operating characteristic (ROC) curve for detecting osteophytes as 0.85. That study, however, had two main limitations. Firstly, the test

set size was relatively small compared to the other OA studies^{4,12}. Secondly, the problem of binary discrimination between osteophytes of OARSI grades 0-1 and 2-3 may not be clinically relevant as the grade 1 already indicates the presence of an osteophyte⁶.

In contrast to those studies, the above mentioned limitations were addressed in the recent study by Antony¹⁷ where a CNN-based approach for simultaneous analysis of KL and OARSI grades was proposed. However, the limitation of that study was a dataset that consisted of a combination of MOST (Multi-center Osteoarthritis study) and OAI (Osteoarthritis Initiative) data and, furthermore, the agreements between the method's predictions and the test set labels were shown to be lower than inter-rater agreements between the human observers for KL and OARSI grades. Here, we tackle both of these limitations and demonstrate an excellent agreement of our method with the test set labels.

Other related works to this study are by Antony *et al.*^{12,18} and Tiulpin *et al.*⁴. While the studies by Antony *et al.* were pioneering in the field, the study by Tiulpin *et al.* produced the new state-of-the-art results in KL grading – Cohen's quadratic kappa of 0.83, and also in radiographic OA detection – area under the ROC curve of 0.93. The balanced accuracy was 66.71%.

Contributions

In this study, we present a robust DL-based multi-task framework for automatic simultaneous OARSI and KL scoring, and validate it with an independent test set. The main contributions of this paper can be summarized as follows:

- We demonstrate a possibility to accurately predict individual knee OA features and overall knee OA severity from plain radiographs simultaneously. Our method significantly outperforms previous state-of-the-art approach¹⁷.
- Compared to the previous study¹⁷, for the first time, we utilize two independent datasets for training and testing in assessing automatic OARSI grading: OAI and MOST, respectively.
- We perform an extensive experimental validation of the proposed methodology using various metrics and explore the influence of network's depth, utilization of squeeze-excitation and ResNeXt blocks^{19,20} on the performance, as well as ensembling, transfer learning and joint learning of KL and OARSI grading tasks.
- Finally, we also release the source codes and the pre-trained models allowing full reproducibility of our results.

Materials and Methods

Overview

In this study, we used bilateral posterior-anterior (PA) fixed-flexion knee radiographs as our training and testing material. To pre-process the data, we performed knee joint area localization using random forest regression voting²¹ and applied intensity normalization. Subsequently, utilizing a transfer learning approach²², we initialized a convolutional part of our model from an ImageNet²³ pre-trained model and predicted the KL and OARSI grades simultaneously. The overall pipeline is graphically illustrated in Figure 2.

Data

We utilized two publicly available knee X-ray datasets: OAI (<https://oai.epi-ucsf.org/datarelease/>) and MOST (<http://most.ucsf.edu>). Fixed flexion bilateral Posterior Anterior (PA) images acquired using a Synaflexer positioning frame with the X-ray beam angle of 10° were used in both datasets²⁴.

OAI is a longitudinal study of 4,796 participants examined with X-ray, MRI and other means during 9 follow-up examinations (0 to 96 months). MOST data is a dataset similar to OAI, but acquired from 3,026 participants that were not part of OAI. MOST included 4 follow-up examinations with imaging (0 to 84 months). Both OAI and MOST studies were approved by the institutional review board of the University of California San Francisco and the data acquisition sites. The informed consent was obtained from all the subjects participated in the study. Further details regarding the ethical approvals and methodology of data acquisition can be found by the aforementioned website links.

Data Pre-processing

We performed two types of data pre-processing – on the metadata and image levels. As such, we first removed the data with the missing labels from both OAI and MOST datasets. After filtering out the missing labels (KL and OARSI scorings), we derived a training set of 19,704 knees from OAI dataset and a testing set of 11,743 knees from MOST dataset. Full description of the data is presented in Table 1. A visual representation of distribution of OARSI grades in lateral and medial compartments is presented in Supplementary Figures 2 and 3, respectively.

In contrast to the previous studies^{4,12,17,25}, we applied a different approach to localize the region of interest (ROI). Specifically, we utilized the random forest regression voting approach implemented in a BoneFinder tool²¹ to localize the

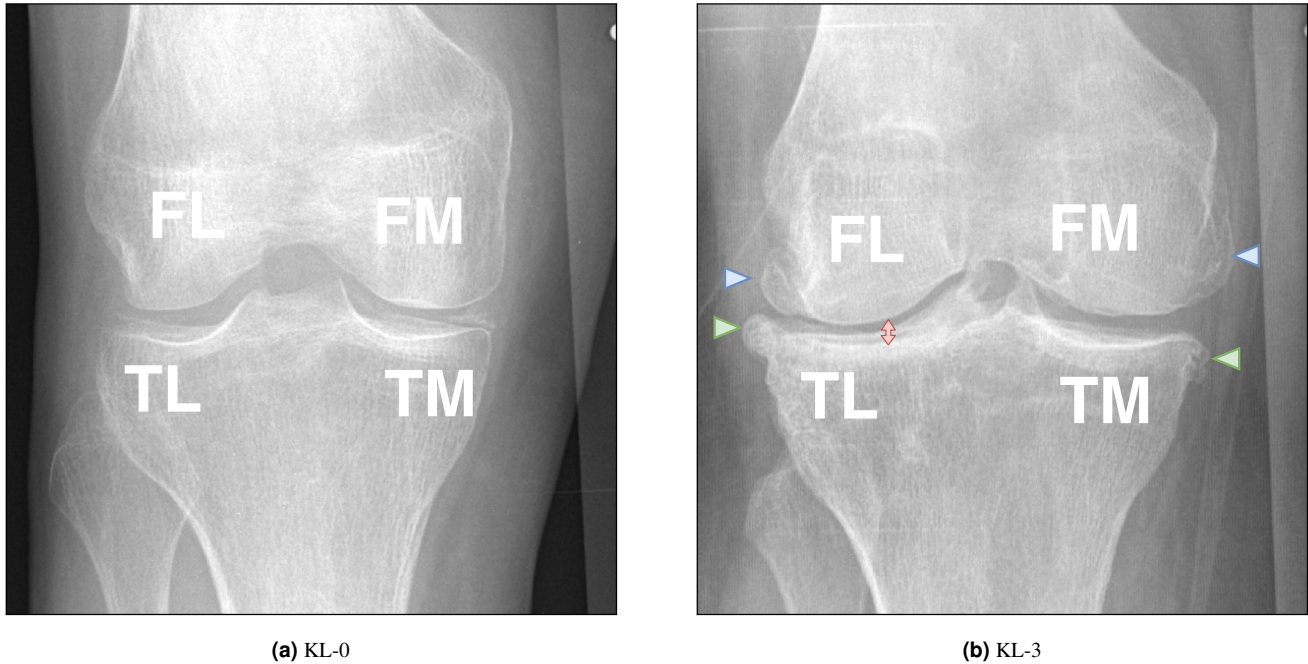


Figure 1. Examples of knee osteoarthritis features graded according to the Osteoarthritis Research Society (OARSI) grading atlas and Kellgren-Lawrence (KL) grading scale. FL, TL, FM and TM represent the femoral lateral, tibial lateral, femoral medial and tibial medial compartments, respectively. In the subplot (a), a right knee without visual OA-related changes is presented (KL 0, all OARSI grades also zero). In the subplot (b), an image of a right knee with severe OA (KL 3) is presented. Blue triangles highlight the osteophytes in femur and the green triangles highlight the osteophytes in tibia. Red arrow highlights the joint-space narrowing (JSN). Here the osteophytes for FL, TL, FM and TM compartments are all of grade 3. JSN in the lateral compartment is of grade 2 and in the medial compartment it is of grade 0.

knee joint landmarks. Subsequently, we cropped the ROIs of 140×140 mm from the right and the left knees, and rotated each individual knee image to horizontally align the tibial plateaus. We also applied histogram clipping and global contrast normalization to each localized knee joint image as proposed in⁴. Finally, we rescaled all the images to 310×310 pixels (0.45 mm resolution) using bilinear interpolation.

Network Architecture

Our approach is based on ensembling of two convolutional neural networks. Each model within the ensemble consists of two parts. The first part is convolutional and was pre-trained on ImageNet²³. The second part consists of 7 independent fully-connected (FC) layers each corresponding to its own task (a KL grade and 6 OARSI grades). To connect these two parts, we utilized an average pooling layer after the convolutional block of our network.

For the convolutional part of the model, we evaluated various network backbones from Resnet family²⁶. As such, we firstly utilized Resnet-18, Resnet-34 and Resnet-50 to assess whether the depth of the model plays any role in predicting OARSI and KL grades in a multi-task setting. Then, we tested the use of squeeze-excitation (SE) blocks by utilizing SE-resnet-50 model architecture¹⁹. Finally, we also used the blocks from ResNeXt model combined with SE modules as proposed in¹⁹.

In addition to the experiments presented in the Results section*, we also evaluated Global Weighted Average Pooling (GWAP)²⁷ instead of a simple average pooling and also GWAP with a hidden layer. Despite being attractive, GWAP and its modification did not lead to improvements on cross-validation. Therefore, we present only the results with the average pooling in the paper.

Training strategy

Our experimental setup employed a 5-fold subject-wise stratified cross-validation. At the model selection phase, we calculated Cohen's kappa coefficients and also the balanced accuracy on out-of-fold sample, thereby utilizing the whole training set. Eventually, we selected two models that performed best in the majority of the tasks and used them in the final ensemble. At the test phase, we performed the inference for each of the model in the ensemble (5 snapshots per model) and eventually averaged

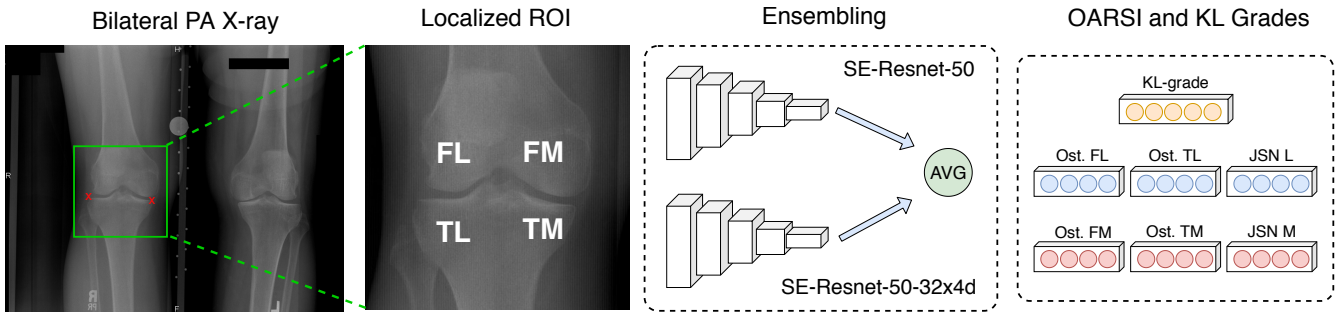


Figure 2. Schematic representation of the workflow of our approach. We use transfer learning from ImageNet and train two deep neural network models, average their predictions and predict totally six knee joint radiographic features according to the OARSIS grading atlas as well as a the KL grade. OARSIS grades for osteophytes in femoral lateral (FL), tibial-lateral (TL), femoral-medial (FM) and tibial-medial (TM) compartments as well as the joint space narrowing (JSN) grades in lateral and medial compartments were predicted.

Table 1. Description of the datasets used in this study. We used all the follow-up examinations from Osteoarthritis Initiative (OAI) and Multi-Center Osteoarthritis Study (MOST). L and M indicate lateral and medial compartments, FO and TO indicate femoral and tibial osteophytes and JSN indicates joint space narrowing, respectively. KL indicates the Kellgren-Lawrence grade.

Dataset	# Images	Grade	# KL	# FO		# TO		# JSN	
				L	M	L	M	L	M
OAI (Train)	19704	0	2,434	11,567	10,085	11,894	6,960	17,044	9,234
		1	2,632	4,698	4,453	5,167	9,181	1,160	5,765
		2	8,538	1,748	2,068	1,169	2,112	1,061	3,735
		3	4,698	1,691	3,098	1,474	1,451	439	970
		4	1,402	-	-	-	-	-	-
MOST (Test)	11743	0	4,899	9,008	7,968	8,596	6,441	10,593	7,418
		1	1,922	1,336	1,218	1,978	3,458	465	1,865
		2	1,838	795	996	647	1,212	442	1,721
		3	2,087	604	1,561	522	632	243	739
		4	997	-	-	-	-	-	-

their predictions.

In all the experiments, we utilized the same training strategy was utilized per type of experiment (with and without transfer learning from ImageNet). Firstly, we performed the transfer learning experiments jointly training to predict both KL and OARSIS grades to select the best network architectures. Secondly, we trained the same models from scratch using the random weight initialization. Thirdly, we also attempted to predict solely OARSIS grades without joint training with KL grade prediction task while still using the ImageNet weights for model initialization.

We executed the transfer learning experiments as follows. For the first two training epochs, only the FC layers were trained with the learning rate (LR) of $1e-2$. Subsequently, we unfroze the convolutional layers and trained the full network with the LR of $1e-3$. Finally, at the beginning of the fourth epoch, we switched to LR of $1e-4$ and trained the models for the remaining seventeen epochs. Adam optimizer was used in all the experiments²⁸.

The training of all the models was regularized using data augmentations from SOLT library²⁹. We used random cropping of 300×300 pixels, Gaussian noise addition and random gamma correction. Besides data augmentations, we also used weight decay of $1e-4$ and dropout of 0.5 (inserted before each FC layer). PyTorch v1.0 was used to train all the models³⁰.

The training of the models from scratch was done with exactly the same hyper-parameters as in the transfer learning experiments besides the starting LR and the LR schedule. As such, the starting LR was $1e-4$ and it was dropped ten times after 10^{th} and 15^{th} epoch.

Finally, it is worth to note that due to data imbalance, we tested various weighted data sampling strategies (e.g. balancing the KL grade distribution as in⁴). However, they did not lead to improvement in the scores.

Table 2. Cross-validation results (out of fold): Cohen’s kappa coefficients for each of the trained tasks on out-of-fold sample (OAI dataset). Best results task-wise are highlighted in bold. We selected two best models for thorough evaluation: SE-Resnet-50[†] and SE-ResNext50-32x4d[‡]. We trained these models from scratch (*) and also with transfer learning, but w/o the KL-grade (**). Finally, in the last row, we show the results for the ensembling of these models. L and M indicate lateral and medial compartments, FO and TO indicate femoral and tibial osteophytes and JSN indicates joint space narrowing, respectively. KL indicates the Kellgren-Lawrence grade.

Backbone	KL	FO		TO		JSN	
		L	M	L	M	L	M
Resnet-18	0.81	0.71	0.78	0.80	0.76	0.91	0.87
Resnet-34	0.81	0.69	0.78	0.80	0.76	0.90	0.87
Resnet-50	0.81	0.70	0.78	0.81	0.78	0.91	0.87
SE-Resnet-50 [†]	0.81	0.71	0.79	0.81	0.78	0.91	0.87
SE-ResNext50-32x4d [‡]	0.81	0.72	0.79	0.82	0.78	0.91	0.87
SE-Resnet-50*	0.78	0.66	0.73	0.76	0.70	0.91	0.87
SE-ResNext50-32x4d*	0.77	0.67	0.73	0.75	0.71	0.91	0.87
SE-Resnet-50**	-	0.71	0.79	0.82	0.78	0.91	0.88
SE-ResNext50-32x4d**	-	0.73	0.80	0.83	0.78	0.91	0.88
Ensemble ^{†‡}	0.82	0.73	0.80	0.83	0.79	0.92	0.88

Results

Cross-validation Results and Backbone Selection

We performed a thorough evaluation of Resnet-18, Resnet-34, Resnet-50, SE-Resnet-50, SE-Resnet-50-32x4d (SE-Resnet-50 with ResNext blocks) using cross-validation (see Table 2 and Supplementary Table 1). Based on cross-validation, we selected two models for further investigation: SE-Resnet-50 and SE-Resnet-50-32x4d. In particular, we investigated the added value of jointly training OARSI and KL grading tasks, added value of transfer learning and, finally, model ensembling. Our experiments indicate that jointly training KL and OARSI grading tasks hurts the performance of automatic OARSI grading. Besides, we found that transfer learning helps significantly for the model convergence. Finally, ensembling two best models allowed to increase the performance in both tasks. Further, we report the results for the ensemble of SE-Resnet-50 and SE-Resnet-50-32x4d as our final model since it yielded the best performance in terms of both – Cohen’s kappa and balanced accuracy (see the latter in Supplementary Table 1).

Test-set Performance

Based on the cross-validation, we selected our final ensemble model to be evaluated on the test set. Its test set performance and also the current state-of-the-art performance reported previously by Antony *et al.* are presented in Table 3. Our method yielded Cohen’s kappa of 0.82 (0.82-0.83) and balanced accuracy of 66.68% (0.66%-0.67%) for KL grading. For OARSI grading tasks, the developed method yielded Cohen’s kappa and balanced accuracy of 0.79 (0.78-0.80) and 63.58% (62.46%-64.84%), 0.84 (0.84-0.85) and 68.85% (68.03%-69.61%), 0.94 (0.93-0.95) and 78.55% (76.70%-80.31%), 0.84 (0.83-0.85) and 65.49% (64.49%-66.47%), 0.83 (0.83-0.84) and 72.02% (70.99%-72.96%) and, finally, 0.90 (0.89-0.90) and 80.66% (79.82%-81.54%) for FO, TO and JSN in lateral and medial compartments, respectively. The 95% confidence intervals here were computed using stratified bootstrapping with 100 iterations.

Besides the metric-based evaluation, we also analysed the confusion matrices for both OARSI and KL grades, as well as the performance of detecting OA, osteophytes presence and abnormal JSN in each knee joint compartment (Figure 3). The confusion matrices for the OARSI grades are presented in Figure 4. Confusion matrix for the KL grading is presented in Supplementary Figure 1.

Discussion

In this study, we developed a DL-based method to perform an automatic simultaneous OARSI and KL grading from knee radiographs using transfer learning. The developed approach employed two deep residual networks with 50 layers that incorporated SE and ResNeXt blocks¹⁹. Compared to the previous state-of-the-art^{4,17}, our model performs significantly better in simultaneous OARSI and KL grading as well as in the detection of radiographic OA presence. The agreement of the predicted OARSI grades on the test set with the test labels exceeds both previously reported human^{17,31} and algorithm¹⁷ performances

Table 3. Test set performance of our ensemble method with SE-Resnet50 and SE-ResNext50-32x4d backbones. F1, MSE, A and K indicate the F1-score (geometric average of precision and recall), mean squared error, balanced accuracy (%) and Cohen’s kappa, respectively. As a comparison, three rightmost columns show the state-of-the-art (SOTA) performance reported by Antony *et al.* in a similar work. L and M indicate lateral and medial compartments, FO and TO indicate femoral and tibial osteophytes and JSN indicates joint space narrowing, respectively. KL indicates the Kellgren-Lawrence grade..

Side	Grade	F1	MSE	A	K	F1 _{SOTA}	A _{SOTA}	K _{SOTA}
L	FO	0.81	0.33	63.58	0.79	0.67	44.3	0.47
	TO	0.83	0.22	68.85	0.84	0.72	47.6	0.52
	JSN	0.96	0.04	78.55	0.94	0.93	69.1	0.80
M	FO	0.81	0.41	65.49	0.84	0.61	45.8	0.48
	TO	0.77	0.26	72.02	0.83	0.66	47.9	0.61
	JSN	0.82	0.20	80.66	0.90	0.75	73.4	0.75
Both	KL	0.65	0.68	66.68	0.82	0.60	63.6	0.69

(see Table 3). Moreover, this is the first study in OA when an independent test set was used for automatic OARSI grading from plain radiographs.

We conducted our experiments in multiple settings: joint training for predicting OARSI and KL grades with and without transfer learning and also prediction of solely OARSI grades without the use of transfer learning. Our results on cross-validation indicate that transfer learning is useful for automatic OARSI grading and also that joint prediction of KL and OARSI grades leads to worse performance. However, the latter is a clinically relevant setting since the KL grade allows for a composite assessment of the knee condition and it is used by practitioners world-wide, in contrast to the OARSI grades. However, OARSI grades allow for evaluation of individual knee features and can be utilized for more comprehensive quantification of OA-related changes between the follow-up examinations when monitoring the OA progression in time. Therefore, despite worse performance, joint prediction of KL and OARSI grades has additional clinical value. In order to overcome the limitations of learning joint KL and OARSI tasks, we performed an ensembling of two models selected using cross-validation – SE-Resnet-50 and SE-ResNext50-32x4d. Our results indicate the notable improvement on cross-validation compared to all the investigated single models (Table 2 and Supplementary Table 1).

This study, while providing the new state-of-the-art results in automatic OARSI grading and detection of radiographic OA presence, has still some limitations. Firstly, compared to the previous work⁴, we did not analyze the attention maps produced by our method. Attention maps could provide further insights into the specific decisions made by the CNN³². However, in this paper we decided to mainly focus on a large-scale experimental evaluation of the conventional transfer learning rather than on model interpretation. Secondly, the presented ensemble approach is computationally heavy due to ensembling and, hypothetically, could affect the real-life use of the developed method unless the model is deployed on GPU. Potentially, techniques like knowledge distillation³³ could help to decrease the computational effort needed for model execution. Thirdly, we utilized the whole knee images for training our models. Future studies should compare this approach with the Siamese model proposed by Tiulpin *et al.*⁴. Fourthly, we considered only the OARSI grades that had sufficient amount of training and test data. Therefore, some additional OARSI features (medial tibial attrition, medial tibial sclerosis and lateral femoral sclerosis) were not considered at all, which could be the target of future studies. Finally, our test set included the data from the same patients obtained from multiple follow-ups. However, this should not significantly affect our results and rather made them less optimistic due to the fact that MOST is a cohort of subjects at risk that have progressing osteoarthritis. Therefore, the appearance of the images changes across the follow-ups and the overall dataset still contains diverse images.

To verify the significance of the last limitation, we made an additional evaluation of the models using only the data from the first imaging follow-up from MOST dataset. We obtained the Cohen’s kappa values of 0.83 (0.82-0.84), 0.79 (0.77-0.81), 0.84 (0.82-0.85), 0.94 (0.93-0.95), 0.86 (0.84-0.87), 0.83 (0.82-0.84), 0.91 (0.90-0.91) for KL as well as for OARSI grades (FO, TO and JSN for lateral and medial compartments), respectively. The balanced accuracy in KL and OARSI grading tasks were of 67.90% (66.57%-69.13%), 64.72 (62.23%-67.16%), 69.11% (66.99%-70.99%), 80% (76.48%-83.21%), 65.80% (63.68%-67.74%), 72.51% (70.40%-74.46%), 83.34% (81.94%-84.64%). Here, the 95%confidence intervals were computed via stratified bootstrapping with 100 iterations. These results are in line with the previous state-of-the-art results for KL grading (kappa of 0.83 and balanced accuracy of 66.71%)⁴ and are significantly better than the results reported by Antony for joint training of KL and OARSI grading tasks (see Table 3).

To conclude, this study demonstrated the first large-scale experiment for automatic KL and OARSI grading. Despite the limitations, we believe that the developed methodology has potential to become a useful tool in clinical OA trials and also

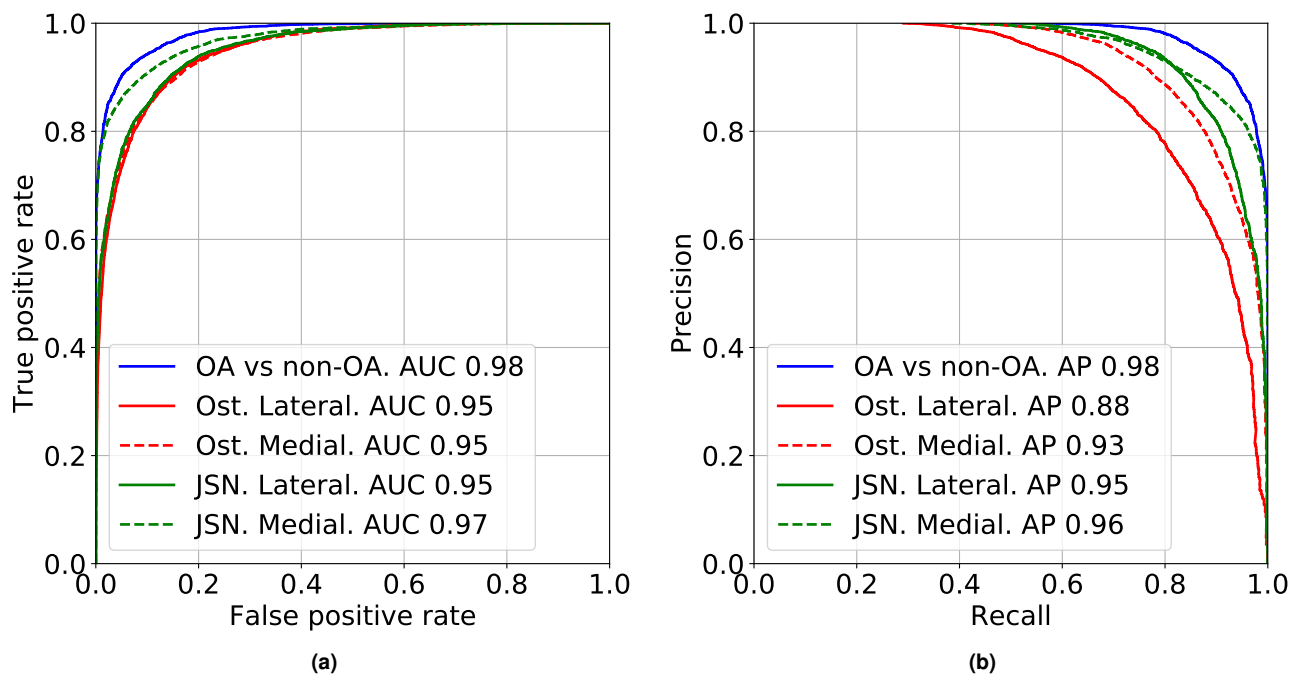


Figure 3. ROC and precision-recall curves demonstrating the performance of detecting the presence of radiographic OA (KL ≥ 2) osteophytes (grade ≥ 1) and joint-space narrowing (grade ≥ 1).

could provide better quantitative information for a clinician in a systematic manner.

Acknowledgments

The OAI is a public-private partnership comprised of five contracts (N01-AR-2-2258; N01-AR-2-2259; N01-AR-2-2260; N01-AR-2-2261; N01-AR-2-2262) funded by the National Institutes of Health, a branch of the Department of Health and Human Services, and conducted by the OAI Study Investigators. Private funding partners include Merck Research Laboratories; Novartis Pharmaceuticals Corporation, GlaxoSmithKline; and Pfizer, Inc. Private sector funding for the OAI is managed by the Foundation for the National Institutes of Health.

MOST is comprised of four cooperative grants (Felson - AG18820; Torner - AG18832; Lewis - AG18947; and Nevitt - AG19069) funded by the National Institutes of Health, a branch of the Department of Health and Human Services, and conducted by MOST study investigators. This manuscript was prepared using MOST data and does not necessarily reflect the opinions or views of MOST investigators.

We would like to acknowledge KAUTE foundation, Sigrid Juselius foundation, Finland, and strategic funding of the University of Oulu. Iaroslav Melekhov is kindly acknowledged for proofreading of the manuscript and Dr. Claudia Lindner is acknowledged for providing BoneFinder tool.

Author contributions

A.T. and S.S. originated the idea of the study. A.T. designed the study, performed the experiments and took major part in writing of the manuscript. S.S. supervised the project. Both authors participated in producing the final manuscript draft and approved the final submitted version.

Competing interests

The authors declare no competing interests.

Data Availability Statement

MOST and OAI datasets are publicly available at <http://most.ucsf.edu/> and <https://oai.epi-ucsf.org/>, respectively. Our dataset splits, source codes and the pre-trained models are publicly available: <https://github.com/MIPT-Oulu/KneeOARSIGrading>.

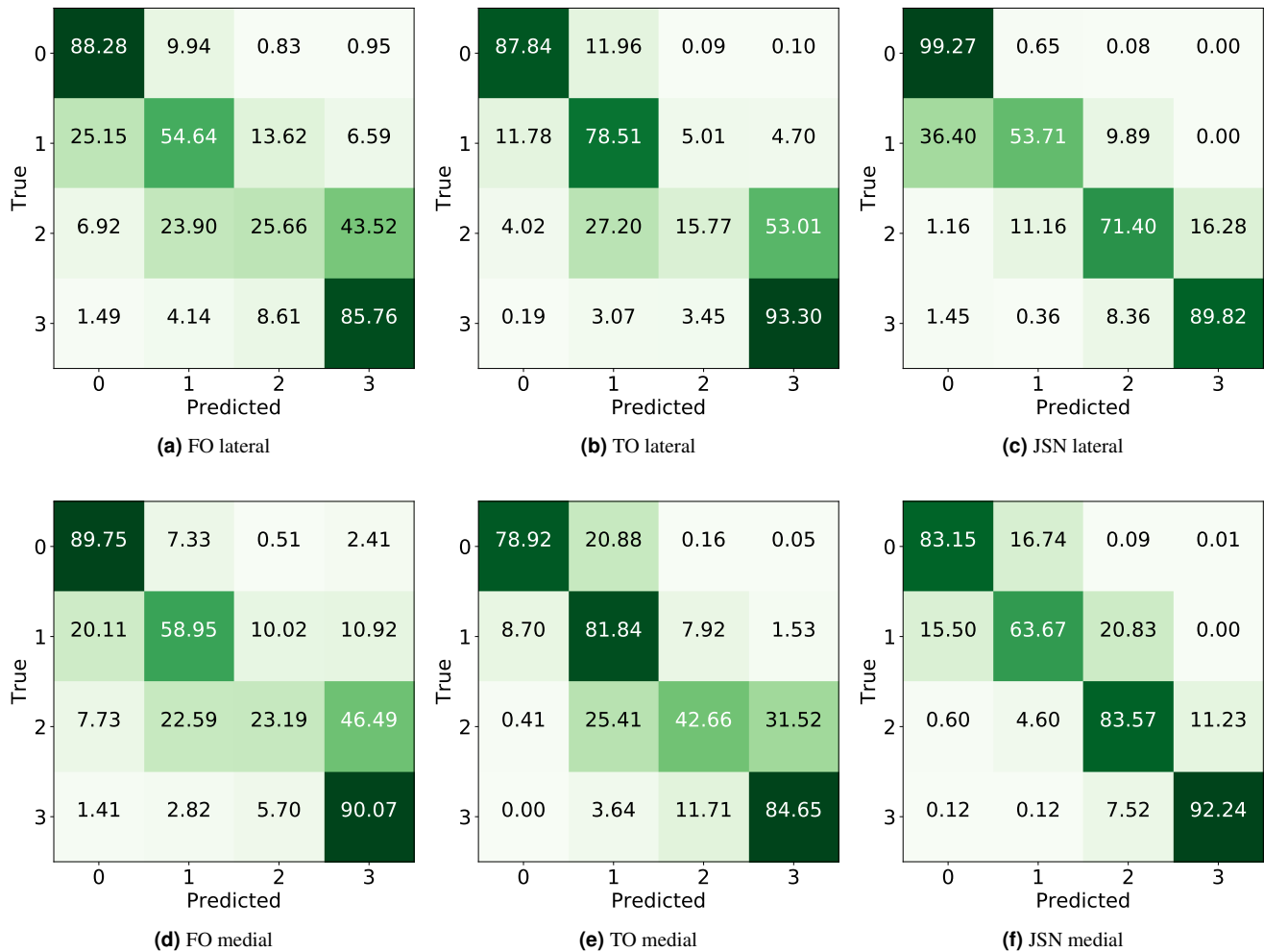


Figure 4. Confusion matrices for the OARSIS grades prediction tasks. The subplots (a)-(c) show the matrices for femoral osteophytes (FO), tibial osteophytes (TO) and joint space narrowing (JSN) automatic grading in lateral compartment and the subplots (d)-(f) show the confusion matrices in the same order, but for the medial compartment. The numbers indicate percentages.

References

1. Arden, N. & Nevitt, M. C. Osteoarthritis: epidemiology. *Best practice & research Clin. rheumatology* **20**, 3–25 (2006).
2. Cross, M. *et al.* The global burden of hip and knee osteoarthritis: estimates from the global burden of disease 2010 study. *Annals rheumatic diseases* **73**, 1323–1330 (2014).
3. Wluka, A. E., Lombard, C. B. & Cicuttini, F. M. Tackling obesity in knee osteoarthritis. *Nat. Rev. Rheumatol.* **9**, 225 (2013).
4. Tiulpin, A., Thevenot, J., Rahtu, E., Lehenkari, P. & Saarakkala, S. Automatic knee osteoarthritis diagnosis from plain radiographs: A deep learning-based approach. *Sci. reports* **8**, 1727 (2018).
5. Kellgren, J. & Lawrence, J. Radiological assessment of osteo-arthrosis. *Annals rheumatic diseases* **16**, 494 (1957).
6. Altman, R. D. & Gold, G. Atlas of individual radiographic features in osteoarthritis, revised. *Osteoarthr. cartilage* **15**, A1–A56 (2007).
7. Esteva, A. *et al.* A guide to deep learning in healthcare. *Nat. medicine* **25**, 24 (2019).

8. Pedoia, V. *et al.* 3d convolutional neural networks for detection and severity staging of meniscus and pfj cartilage morphological degenerative changes in osteoarthritis and anterior cruciate ligament subjects. *J. Magn. Reson. Imaging* **49**, 400–410 (2019).
9. Norman, B., Pedoia, V. & Majumdar, S. Use of 2d u-net convolutional neural networks for automated cartilage and meniscus segmentation of knee mr imaging data to determine relaxometry and morphometry. *Radiology* **288**, 177–185 (2018).
10. Tiulpin, A., Finnilä, M., Lehenkari, P., Nieminen, H. J. & Saarakkala, S. Deep-learning for tidemark segmentation in human osteochondral tissues imaged with micro-computed tomography. *arXiv preprint arXiv:1907.05089* (2019).
11. Tiulpin, A. *et al.* Multimodal machine learning-based knee osteoarthritis progression prediction from plain radiographs and clinical data. *arXiv preprint arXiv:1904.06236* (2019).
12. Antony, J., McGuinness, K., Moran, K. & O'Connor, N. E. Automatic detection of knee joints and quantification of knee osteoarthritis severity using convolutional neural networks. In *International conference on machine learning and data mining in pattern recognition*, 376–390 (Springer, 2017).
13. Norman, B., Pedoia, V., Noworolski, A., Link, T. M. & Majumdar, S. Applying densely connected convolutional neural networks for staging osteoarthritis severity from plain radiographs. *J. digital imaging* 1–7 (2018).
14. Xue, Y., Zhang, R., Deng, Y., Chen, K. & Jiang, T. A preliminary examination of the diagnostic value of deep learning in hip osteoarthritis. *PloS one* **12**, e0178992 (2017).
15. Oka, H. *et al.* Normal and threshold values of radiographic parameters for knee osteoarthritis using a computer-assisted measuring system (koacad): the road study. *J. Orthop. Sci.* **15**, 781–789 (2010).
16. Thomson, J., O'Neill, T., Felson, D. & Cootes, T. Detecting osteophytes in radiographs of the knee to diagnose osteoarthritis. In *International Workshop on Machine Learning in Medical Imaging*, 45–52 (Springer, 2016).
17. Antony, A. J. *Automatic quantification of radiographic knee osteoarthritis severity and associated diagnostic features using deep convolutional neural networks*. Ph.D. thesis, Dublin City University (2018).
18. Antony, J., McGuinness, K., O'Connor, N. E. & Moran, K. Quantifying radiographic knee osteoarthritis severity using deep convolutional neural networks. In *2016 23rd International Conference on Pattern Recognition (ICPR)*, 1195–1200 (IEEE, 2016).
19. Hu, J., Shen, L. & Sun, G. Squeeze-and-excitation networks. In *Proceedings of the IEEE conference on computer vision and pattern recognition*, 7132–7141 (2018).
20. Xie, S., Girshick, R., Dollár, P., Tu, Z. & He, K. Aggregated residual transformations for deep neural networks. In *Proceedings of the IEEE Conference on Computer Vision and Pattern Recognition*, 1492–1500 (2017).
21. Lindner, C. *et al.* Fully automatic segmentation of the proximal femur using random forest regression voting. *IEEE transactions on medical imaging* **32**, 1462–1472 (2013).
22. Shin, H.-C. *et al.* Deep convolutional neural networks for computer-aided detection: Cnn architectures, dataset characteristics and transfer learning. *IEEE transactions on medical imaging* **35**, 1285–1298 (2016).
23. Deng, J. *et al.* ImageNet: A Large-Scale Hierarchical Image Database. In *CVPR09* (2009).
24. Kothari, M. *et al.* Fixed-flexion radiography of the knee provides reproducible joint space width measurements in osteoarthritis. *Eur. radiology* **14**, 1568–1573 (2004).
25. Tiulpin, A., Thevenot, J., Rahtu, E. & Saarakkala, S. A novel method for automatic localization of joint area on knee plain radiographs. In *Scandinavian Conference on Image Analysis*, 290–301 (Springer, 2017).
26. He, K., Zhang, X., Ren, S. & Sun, J. Deep residual learning for image recognition. In *Proceedings of the IEEE conference on computer vision and pattern recognition*, 770–778 (2016).
27. Qiu, S. Global weighted average pooling bridges pixel-level localization and image-level classification. *arXiv preprint arXiv:1809.08264* (2018).
28. Kingma, D. P. & Ba, J. Adam: A method for stochastic optimization. *arXiv preprint arXiv:1412.6980* (2014).
29. Tiulpin, A. Solt: Streaming over lightweight transformations. <https://github.com/MIPT-Oulu/solt> (2019).
30. Paszke, A. *et al.* Automatic differentiation in pytorch. In *NIPS-W* (2017).
31. Riddle, D. L., Jiranek, W. A. & Hull, J. R. Validity and reliability of radiographic knee osteoarthritis measures by arthroplasty surgeons. *Orthopedics* **36**, e25–e32 (2013).

32. Ching, T. *et al.* Opportunities and obstacles for deep learning in biology and medicine. *J. The Royal Soc. Interface* **15**, 20170387 (2018).
33. Hinton, G., Vinyals, O. & Dean, J. Distilling the knowledge in a neural network. *arXiv preprint arXiv:1503.02531* (2015).

Supplementary data

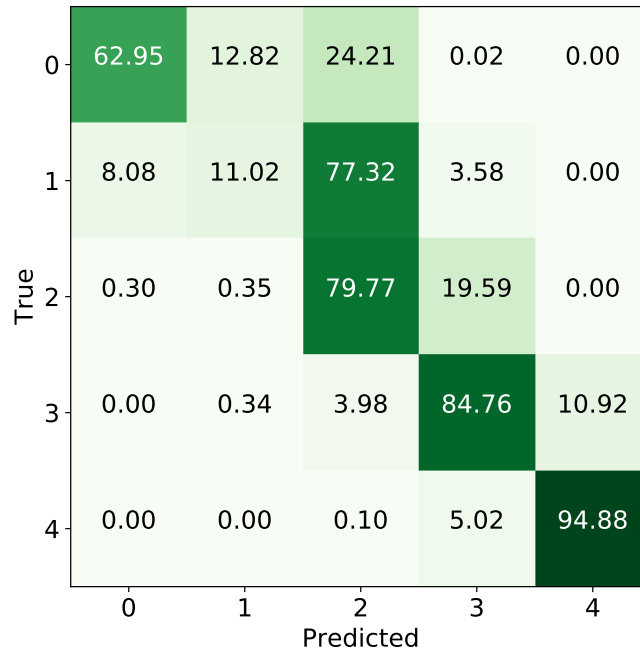


Figure 1. Confusion matrix for Kellgren-Lawrence (KL) grading. The numbers indicate percentages.

Table 1. Cross-validation results (out of fold): balanced accuracy (%) for each of the trained tasks on out-of-fold sample (OAI dataset). Best results task-wise are highlighted in bold. We selected two best models for through evaluation: SE-Resnet-50[†] and SE-ResNext50-32x4d[‡]. We trained these models from scratch (*) and also with transfer learning, but w/o the KL-grade (**). Finally, in the last row, we demonstrate the results for the ensembling of these models. L and M indicate lateral and medial compartments, FO and TO indicate femoral and tibial osteophytes and JSN indicates joint space narrowing, respectively. KL indicates the Kellgren-Lawrence grade.

Backbone	KL	FO		TO		JSN	
		L	M	L	M	L	M
Resnet-18	67.32	53.19	61.08	60.37	62.38	75.74	77.92
Resnet-34	66.93	50.91	60.11	61.86	62.13	73.66	79.09
Resnet-50	66.99	52.35	62.57	61.93	64.40	73.42	78.95
SE-Resnet-50 [†]	67.77	53.96	62.54	63.22	65.24	76.13	78.22
SE-ResNext50-32x4d [‡]	67.08	55.37	63.31	64.55	65.14	75.05	78.65
SE-Resnet-50*	65.07	48.58	54.64	56.14	56.44	75.86	78.56
SE-ResNext50-32x4d*	64.31	49.25	55.11	56.04	56.76	75.58	78.89
SE-Resnet-50**	-	54.97	63.28	64.00	64.17	73.39	79.65
SE-ResNext50-32x4d**	-	55.40	63.84	66.26	65.00	74.81	78.90
Ensemble ^{†‡}	68.01	55.15	63.86	64.83	65.70	76.73	79.03

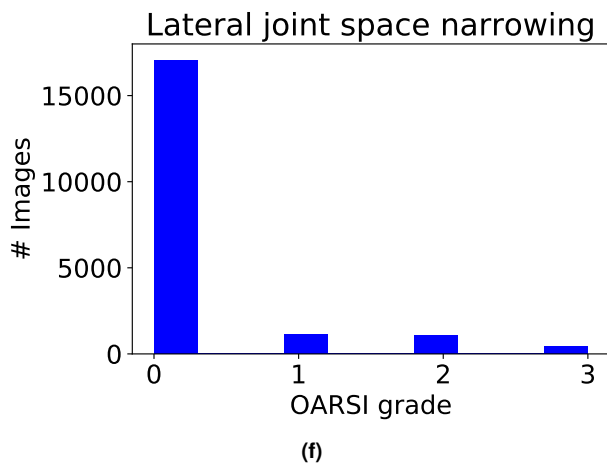
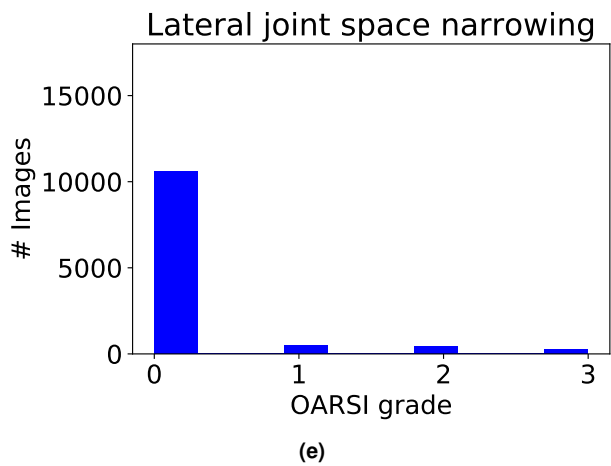
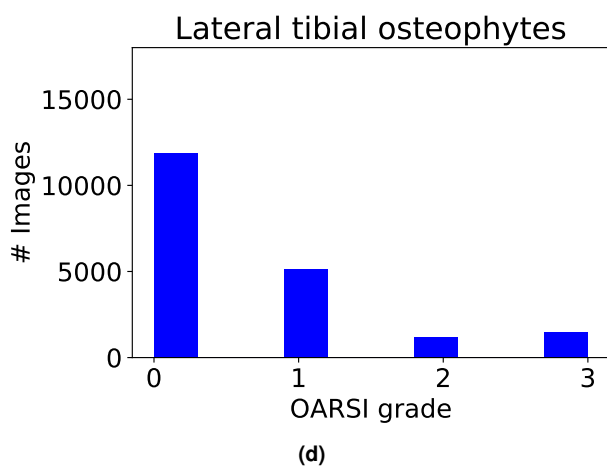
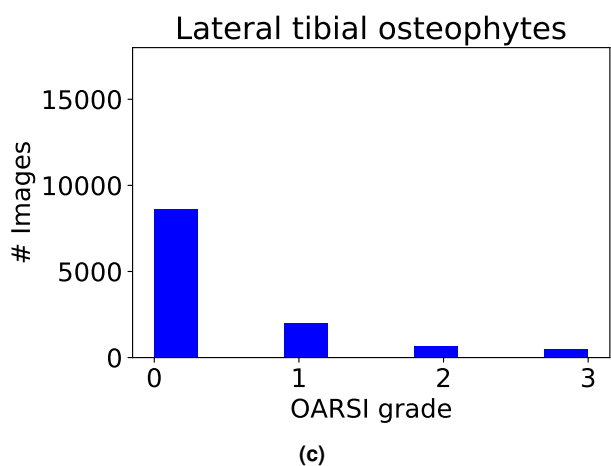
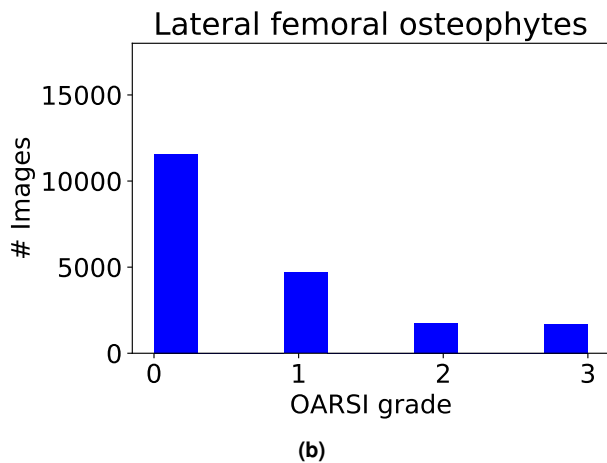
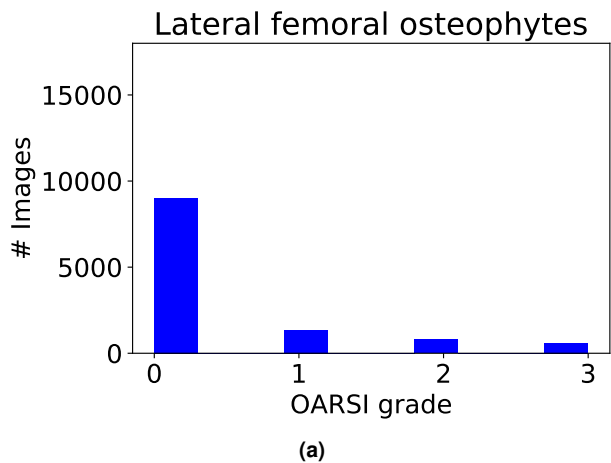
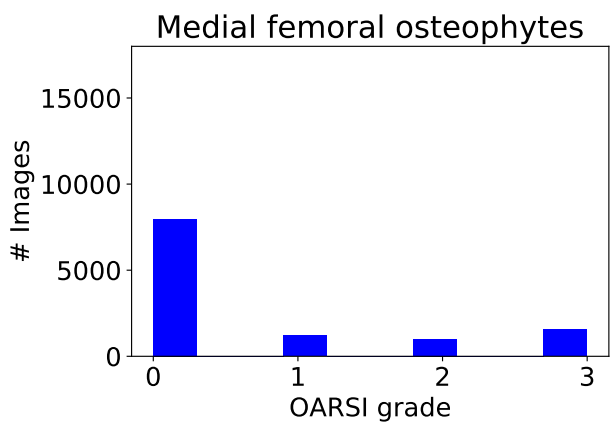
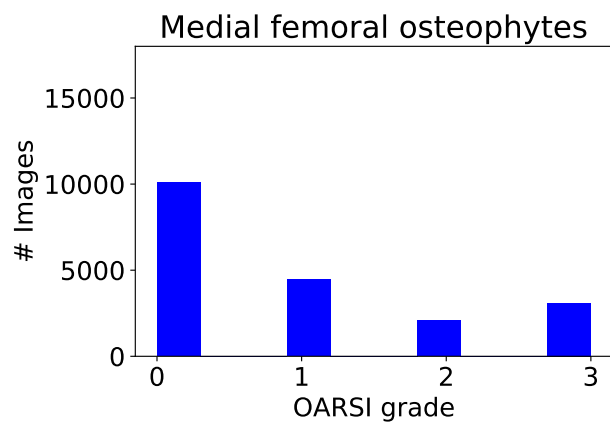


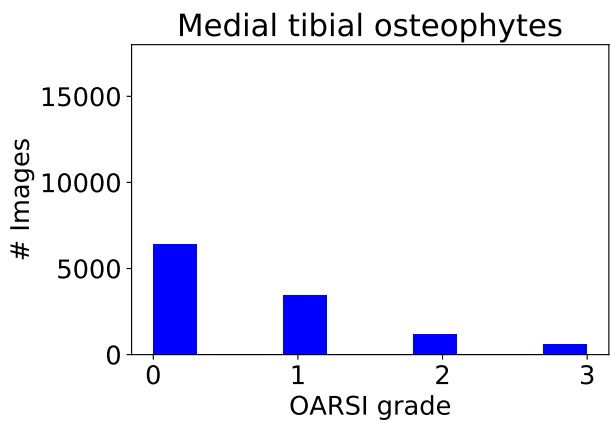
Figure 2. Visual representation of lateral OARSI grades distributions in MOST (2a, 2c, 2e) and OAI (2b, 2d, 2f) datasets.



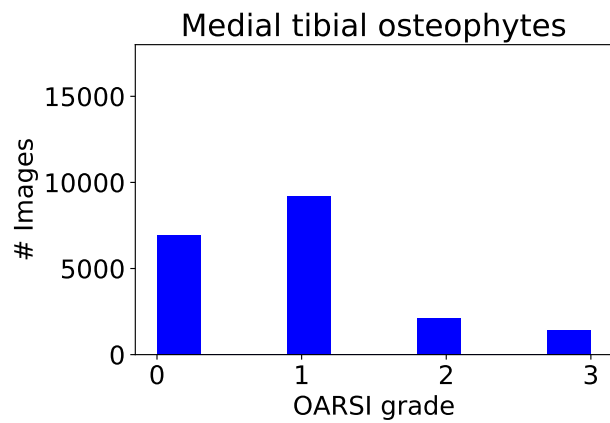
(a)



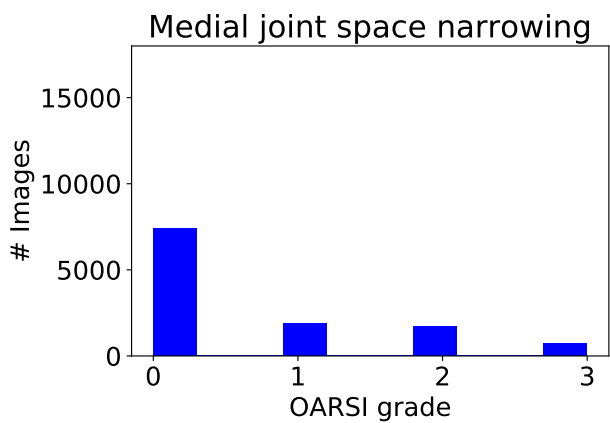
(b)



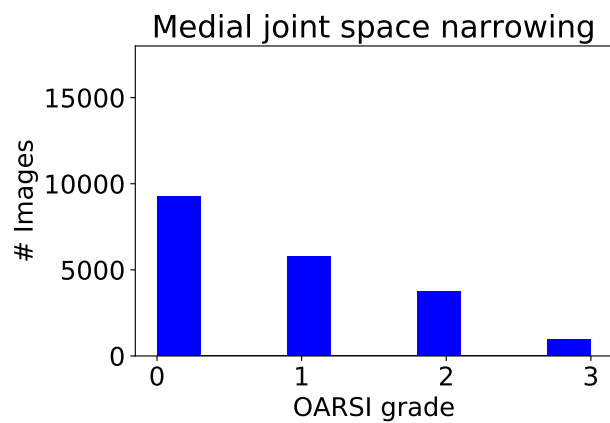
(c)



(d)



(e)



(f)

Figure 3. Visual representation of lateral OARSI grades distributions in MOST (3a, 3c, 3e) and OAI (3b, 3d, 3f) datasets.